IOSR Journal of Applied Geology and Geophysics (IOSR-JAGG)
e-ISSN: 2321–0990, p-ISSN: 2321–0982.Volume 10, Issue 1 Ser. III (Jan. – Feb. 2022), PP 15-24
www.iosrjournals.org

Determination of Local Quasi-Geoid Models using FFT Estimation Technique based on Combined Gravity Anomalies from CHAMP, GRACE, GOCE, Future Satellite Missions and in-Situ Gravity observations in Western Desert of Egypt

Basem Elsaka[1,2], Mohamed El-Ashquer[3]
[1](*Astronomical, Physical and Mathematical Geodesy (APMG) Department, Institute of Geodesy and Geoinformation, University of Bonn, Bonn, Germany)*
[2](*Geodynamics Department, National Research Institute of Astronomy and Geophysics (NRIAG), Helwan, Cairo, Egypt)*
[3](*Construction Engineering and Utilities Department, Faculty of Engineering, Zagazig University, Zagazig, Egypt)*
Corresponding author: Basem Elsaka

Abstract:
Determination of gravity field from space has been successfully improved during the last two decades by launching satellite gravity missions. In this contribution, numerous gravimetric quasi-geoid models are determined from ground-truth gravity anomalies of the past (CHAMP, GRACE and GOCE) and future (e.g. Bender-type, Cartwheel-type, Helix-type and Pendulum-type) satellite gravity missions combined with ground-based terrestrial free-air anomalies over a selected zone of the Western Deseret of Egypt between 23°N to 27°N and from 30°E to 32°E as a case study. Regarding to the methodology, the fast Fourier transformation (1D-FFT) method will be implemented. The findings over a selected zone of the Egyptian Western Desert show a superiority of the future gravity missions, particularly the Bender-type in modelling the local quasi-geoid heights providing the least standard deviations (st. dev.) in terms of residual quasi-geoid heights of about 32.571 cm w.r.t. the past gravity missions (CHAMP, GRACE and GOCE), which provide st. dev. ranging between 32.64 to 36.51 cm.

Key Words: *Past and Future satellite gravity missions; Free-air gravity anomalies; Fast Fourier transformation (1D-FFT); Local quasi-geoid determination.*

Date of Submission: 13-02-2022 Date of Acceptance: 28-02-2022

I. Introduction

The recovering the Earth's gravity field from space has been realized by the launch of the Challenging Minisatellite Payload (CHAMP) mission (2000 – 2010) (Reigber, 1989). This mission characterized by a low and near-polar orbit of initial altitude of 454 km and inclination of 87°, and an on-board accelerometer to measure the non-gravitational forces (e.g. air drag and solar radiation pressure). Through the continuous tracking of CHAMP satellite from GPS (Global Positioning System) satellites simultaneously, an almost uninterrupted determination of the long-wavelength gravitational field could be achieved with a spatial resolution of about 133 km representing spherical harmonics (SH) degree and order (d/o) 150/150 (Flechtner et al., 2010). Between 2002 and 2017, successful collaboration of the U.S. National Aeronautics and Space Administration (NASA) and the German Aerospace Centre (DLR), was conceived (Tapley et al., 2004) to launch the dual-satellite mission Gravity Recovery and Climate Experiment (GRACE). Unlike CHAM, the principle of GRACE was advanced by combining the high-low SST from GPS satellite with a high precision low-low SST system (i.e. between the dual-GRACE satellites) allowing the determination of the Earth's gravity field with a considerably accuracy around 1×1 degree (i.e. ≈111 km) which was higher than that achieved by the CHAMP mission. The twin GRACE satellites provided for the first time the gravity field's temporal variations within time intervals of about 30 days. The dedicated satellite mission GOCE (Gravity Field and Steady-State Ocean Circulation Explorer) was selected as the first core mission within the Living Planet Earth Observation Programme of the Earopean Space Agency (ESA, 1999). It was successfully launched between 2009 and 2013 with a lower altitude than CHAMP and GRACE of about 260 km and an orbital inclination of 96.5°. The main

payload of GOCE consisted of a GPS receiver and the gravity gradiometer consisting of 6 accelerometers mounted on 3 axes in perpendicular directions to measure in-orbit gravity gradient. The gradiometry measurements had already improved the determination of the static geoid height with an accuracy of 1 to 2 cm at a spatial scale of 100 km.

Further improvements have been achieved using different satellite configurations as studied by Sharifi et al., 2007, Sneeuw et al., 2008; Bender et al., 2008; Wiese et al., 2009; Elsaka, 2010; Anselmi et al., 2011; Wiese et al., 2011; Wiese et al., 2012; Elsaka et al., 2012, Elsaka et al., 2014; Daras et al., 2014; Elsaka et al., 2015; Iran Pour et al., 2015; Flechtner et al. 2016, Pail et al. 2018; Nie et al., 2019 and Elsaka, 2019, Haagmans et al., 2020). For instance, Figure 1 shows four proposed future mission scenarios; the Bender-, Cartwheel-, Helix- and Pendulum-types, which have inter-satellite link in different flight directions (along-track, cross-track and radial). For detailed description, the reader is referred to Elsaka et al., (2014).

The goal of this work is to model the local quasi-geoid heights from satellite-based observations, in particularly, from previous (CHAMP, GRACE and GOCE) and future (Bender, Cartwheel, Helix and Pendulum) satellite gravity missions. In this paper, we compute local quasi-geoid heights in a selected area of the Egyptian Western Desert bounded between 23°N to 27°N and from 30°E to 32° E as a case study based on combined free-air gravity anomalies from satellite and ground-truth observations using the 1D-FFT Estimation Technique (Heiskanen and Moritz, 1967). For this purpose, the GRAVSOFT software package (Forsberg and Tscherning, 2008) has been used. In the following, the datasets used in our calculations are briefly described in Section II. In Section III, methodology for computing the height anomalies are represented. The results are discussed in Section IV. Finally, conclusions are outlined in Section V.

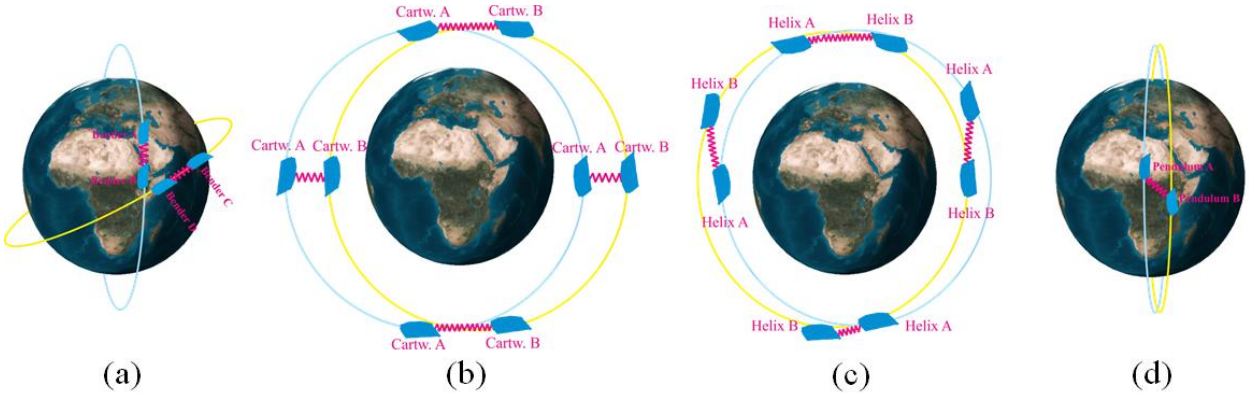

Figure 1. Investigated future gravity satellite missions (a) Bender-type, (b) Cartwheel-type, (c) Helix-type and (d) Pendulum-type (after Elsaka et al., 2014).

II. Datasets

The datasets used in this study consist of : (1) The in-situ terrestrial free-air gravity anomalies located in the area between 23°N to 27°N and from 30°E to 32°E in the Western Deseret of Egypt; (2) The geopotential spherical harmonics (SH) up to d/o 120 from all aforementioned (previous and future) satellite gravity missions and (3) High-resolution topographic data from the SRTM30_PLUS (Shuttle Radar Topography Mission) digital terrain model as given via the website http://topex.ucsd.edu/cgi-bin/get_srtm30.cgi. These datasets are required to compute the gravimetric height anomalies through the remove-restore principle (see Hofmann and Moritz, 2005, p. 379)In the following, the applied datasets within this paper are discussed.

II.1. In-situ Free-air Gravity Data

Regarding the in-situ free-air gravity data, 154 point gravity stations were available in this study as provided by the National Research Institute of Astronomy and Geophysics (NRIAG) (private communication). These dataset has been observed using two Lacoste & Romberg gravimeters of models "G" and "D" of reliability and accuracy of about $10\mu Gal$ and $1\mu Gal$ $(1\,\mu Gal = 10^{-8}\,m/s^2)$, respectively. The distribution of gravity data is so far homogeneous over selective area in Western Desert of Egypt covering latitude from 23°N to 27°N and longitude from 30°E to 32°E. Figure 2 shows the distribution of available in-situ free-air gravity data of the study area over topographic and bathymetric map of Egypt. In addition, rapid static GPS observations were accompanied at each of the gravity stations in order to determine its location. The statistical properties of the free-air anomalies can be seen in Table 1.

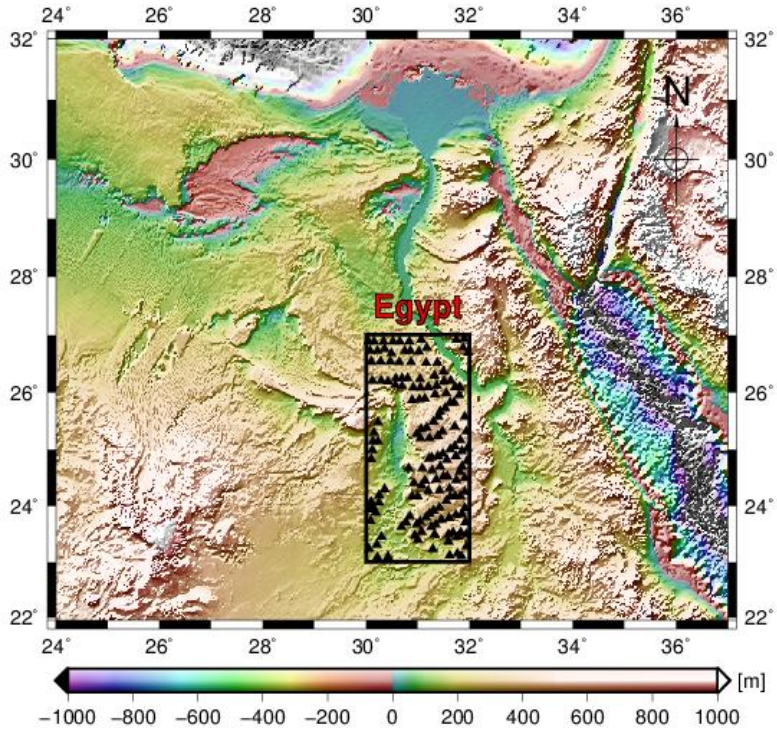

Figure 2. Distribution of available in-situ free-air gravity data of the study area over topographic and bathymetric map in [m] as deduced from SRTM30_PLUS data.

Table 1. Statistics of the in-situ free-air gravity anomalies.

Statistics	Min	Max	Mean	st. dev.
Fa	-102.69	96.13	-0.039	24.97

II.2. Geopotential Gravity Models (GGM)

A large number of satellite-based geopotential gravity models (GGMs) have been developed during the last two decades (from the early 2002 till now). They are available via the International Centre for Global Earth Model ICGEM website; http://icgem.gfz-potsdam.de/tom_longtime. In this study, the long wavelength spectrum (up to d/o 120) has been truncated from several GGMs based on datasets of the three satellite gravity missions; CHAMP, GRACE and GOCE. These models are CHAMP-based ulux_champ2013s, GRACE-based ITG-GRACE2010s and GOCE-based GO_CONS_GCF_2_SPW_R5 (SPW5), GO_CONS_GCF_2_DIR_R6 (DIR6) and GO_CONS_GCF_2_TIM_R6 (TIM6). In addition, the long wavelength spectrum of four simulated gravity models of future gravity missions; namely Bender-, Cartwheel-, Helix- and Pendulum-type have been taken from Elsaka et al., (2014).

II.3. Topography Data

The topographic potential effects required for modelling the gravimetric geoid heights have been computed based on data of the SRTM30_PLUS (Shuttle Radar Topography Mission of spatial resolution about ~900 m, 30 arc-sec) given via the website http://topex.ucsd.edu/cgi-bin/get_srtm30.cgi. The topographic heights in meters used for our modelling process as deduced from the SRTM30_PLUS data over Egypt as shown in Figure 2.

II.4. Combined Data

Since the in-situ gravity anomalies obtained from terrestrial measurements contain 'theoretically' the full spectral information of the gravity field, particularly the high- and very-high-frequency ranges, which are not included in the GGMs given in Sec. 2.2, so the spectral consistency should be taken into consideration. This is due to the fact that gravity anomalies provided by the GGMs have a finite wavelength range of the gravity spectrum. For this reason, we add the contribution of the short and very-short wavelength gravity signals beyond the applied maximum degree (i.e. d/o 120) of GGMs using the Eigen-6C4 [26] up to d/o 720. The choice of applying d/o 720 is due to the fact that the Eigen-6C4 is based on the reconstruction of the EGM2008 (Pavlis et al. 2012), which takes into account the "fill-in" technique for regions with poor gravity data set coverage, such as the Western Desert area of Egypt, where our dataset is located. Because the "fill-in" technique seems to be

unable to improve the EGM2008 beyond d/o 720 over the study area. So, the GGMs given in Sec. 2.2 have been extended based on Eigen-6C4 from 121 up to 720, and hence, applied for our modelling purpose. The omitted gravity signal from d/o 721 onward has been then estimated from the topography data (see Sec. 2.3). Accordingly, the in-situ free-air anomalies could be then compared with the extended GGMs noting here that the differences in all extended geopotential models are only in the long wavelength of gravity spectrum which is the main investigation scope of this study.

III. Methodology

In order to get the residual height anomalies from the terrestrial free air gravity anomalies, the fast Fourier transformation (1D-FFT) method has been applied. In this technique, the residual height anomalies ζ_{res} have been calculated from the residual gravity anomalies $\Delta g_{res(I)}$ first by gridding gravity anomalies. Correspondingly, the Stokes integral with 1D-FFT technique has been applied as (Heiskanen and Moritz, 1967) as:

$$\zeta_{\varphi I}(\lambda) = \frac{R\Delta\varphi\Delta\lambda}{4\pi\lambda} F_1^{-1} \sum_{\varphi_J} F_1\left(\Delta g_{res(I)} \cos\varphi_I\right) F_1\left[S\left(\lambda_I - \lambda_J\right)\right] \quad (1)$$

Where and F_1 and F_1^{-1} stand for the one-dimensional Fourier transform and its inverse, respectively. Accordingly, the Wong Gore modification (Wong and Gore, 1969) has been applied, where the lowest harmonics are set to zero up to maximum degree (N) as:

$$S_{mod}(\psi) = S(\psi) - \sum_{n=2}^{N} \alpha(n) \frac{2n+1}{n-1} P_n \cos\psi \quad (2)$$

with

$$\alpha(n) = \begin{cases} 0 & for\ n > N \\ 1 & for\ 2 \le n \le N \end{cases} \quad (3)$$

Where S_{mod} and S are the modified and original Stokes' kernel functions, respectively. So, the residual height anomalies ζ_{res} have been calculated from residual gravity anomalies similar to Saadon et al., (2021) who used the 1D-FFT method (Equation 1) applying the SP1D program (Forsberg and Tscherning, 2008).

IV. Results

Nine gravimetric quasigeoid models are determined from the investigated satellite-based models of CHAMP-based ulux_champ2013s, GRACE-based ITG-GRACE2010s, GOCE-based DIR_R6, TIM_R6 and SPW_R5, Bender-type, Cartwheel-type, Helix-type and Pendulum-type. As mentioned in Sec. 2.4., these models have been modified using the Eigen-6C4 in order to compare their gravity anomalies with the corresponding terrestrial gravity anomalies as follows:

$$\Delta g_{GGM\_mod} = \Delta g_{GGM}|_2^{120} + \Delta g_{Eigen\text{-}6C4}|_{121}^{720} \quad (4)$$

The remove-restore procedure, as one of most commonly applied methods in physical geodesy, has been applied. At first step, the remove step, the long and short wavelength spectra of the gravity signal as determined in Equation (4) was removed from the in-situ free-air gravity anomalies (Δg_{Fa}). In addition, the gravity effect due to the topographic attraction, representing the very-short wavelength component, has been evaluated with the residual terrain model (RTM) reduction (Δg_{RTM}) from the raw gravity anomalies (Δg_{Fa}) to compute finally the resulting residual anomalies (Δg_{res}) as:

$$\Delta g_{res} = \Delta g_{Fa} - \Delta g_{GGM\_mod} - \Delta g_{RTM} \quad (5)$$

The FFT process (Equation 1) has been applied to compute the residual height anomalies (ζ_{res}). This step is done applying the SP1D module of GRAVSOFT software package (Forsberg and Tscherning, 2008) similar to the calculations done by Saadon et al. (2021). In the restore step, the long as well as short wavelength spectra in terms of height anomalies is added to the residual height anomalies to estimate the gravimetric quasigeoid heights as

$$\zeta = \zeta_{res} + \zeta_{GGM} + \zeta_{RTM} \quad (6)$$

Table 2 shows the statistics of the first part of Equation (5) representing the difference of gravity anomalies after the removal of the long and short wavelength spectra. It shows clearly that when removing the long and short wavelength components ($\Delta g_{GGM\_mod}|_2^{720}$) from the free-air gravity anomalies (Δg_{Fa}), substantial smoothing is provided as given by the reduction of standard deviations (st. dev.) especially those provided by the future satellite missions of about 24.37 mGal.

Table 2. Statistics of gravity anomalies [mGal] after the removal of the long and short wavelength gravity spectra (i.e. $\Delta g_{Fa} - \Delta g_{GGM\_mod}$)

GGM	Min	Max	Mean	st. dev.
Ulux_champ2013s	-128.694	62.440	-4.8452	25.57334
ITSG_GRACE2018s	-120.400	57.600	-4.5152	24.39963
DIR6	-120.401	57.612	-4.5198	24.39994
SPW5	-120.379	57.589	-4.4836	24.39988
TIM6	-120.449	57.582	-4.5060	24.40358
Bender-type	-120.178	57.938	-4.6208	24.37726
Cartwheel-type	-120.186	57.930	-4.6248	24.37792
Helix-type	-120.181	57.936	-4.6173	24.37760
Pendulum-type	-120.184	57.943	-4.6251	24.37773

After the removal of the very-short wavelength components due to local topography, slight reduction in terms of standard deviations (st. dev.) reached to about 0.18 mgal of the residual gravity (Δg_{res}) were obtained as given in Table 3. These slight refinements might be due to the flatness of the study area of the Western Desert, where the topography is very smooth. This can be seen in Figure 3, which shows the obtained residual gravity anomalies represented by Equation (5).

Table 3. Statistics of residual gravity anomalies [mGal] after the removal of the very-short wavelength gravity spectrum (i.e. Δg_{res})

GGM	Min	Max	Mean	st. dev.
Ulux_champ2013s	-128.018	63.432	-5.3167	25.40913
ITSG_GRACE2018s	-119.724	58.592	-4.9866	24.22175
DIR6	-119.725	58.603	-4.9912	24.22204
SPW5	-119.703	58.581	-4.9550	24.22158
TIM6	-119.773	58.574	-4.9775	24.22551
Bender-type	-119.503	58.930	-5.0923	24.19785
Cartwheel-type	-119.510	58.921	-5.0962	24.19857
Helix-type	-119.505	58.927	-5.0888	24.19824
Pendulum-type	-119.508	58.935	-5.0965	24.19836

To apply the 1D-FFT technique applying the SP1D-program, the residual free-air gravity anomalies (Equation 5) are interpolated on a grid of 0.25° x 0.25° resolution. The gridded residual free-air gravity anomalies over the selected zone of the Western Desert of Egypt have been converted to the residual geoid heights (ζ_{res}) applying the wong-gore modification of stokes' integral from zero up to maximum spherical harmonics degree, which was 120 in our study. The results are given in Table 4 in terms of standard deviations of the residuals of gravimetric quasi-geoid heights. It should be noted here that we represent only the residuals indicated by the first term in the right hand side of Equation (6) in order to see the discrepancies between the solutions without the effect of the long (represented by the Eigen-6C4) as well as the very-short (RTM) gravity signals. The results are seen spatially in Figure 4.

Regarding the previous gravity missions, the CHAMP-based model (ulux_champ2013s) approximates the quasi-geoid over the Western Desert in worse manner providing st. dev. of about 36.51 cm w.r.t. the GRACE solution (ITSG-GRACE2018s) which provides st. dev. of about 32.62 cm and GOCE solutions (DIR6, SPW5 and TIM6), which provide st. dev. between 32.62 cm and 32.64 cm. Regarding the proposed four future satellite missions, one can clearly see that their residual estimates of quasi-geoid heights surpass the other estimates provided by the past gravity missions providing the st. dev. of about 32.57 cm. In particular, the Bender-type provides the most promising solution and shows superiority in modelling the local gravimetric quasi-geoid heights over the study area. In fact, this is expected since the observations of Bender-type mission configuration carry additional cross-track information besides the along-track one. To sum up, modelling of local gravimetric quasi-geoid heights needs more concern not only by considering the improvement of the short wavelengths but also by involving the most promising long wavelength into the modelling process that can be acquired from the launch of future gravity missions.

Table 4. Statistics of residual geoid heights anomaly ζ_{res} (m)

GGM	Min	Max	Mean	st. dev.
Ulux_champ2013s	-1.055	0.877	0.05799	0.36512
ITSG_GRACE2018s	-0.937	0.815	0.04970	0.32622

DIR6	-0.938	0.816	0.04958	0.32623
SPW5	-0.939	0.814	0.04991	0.32639
TIM6	-0.939	0.814	0.04980	0.32643
Bender -type	-0.942	0.823	0.04841	0.32571
Cartwheel-type	-0.942	0.823	0.04837	0.32573
Helix-type	-0.942	0.823	0.04848	0.32572
Pendulum -type	-0.942	0.823	0.04844	0.32573

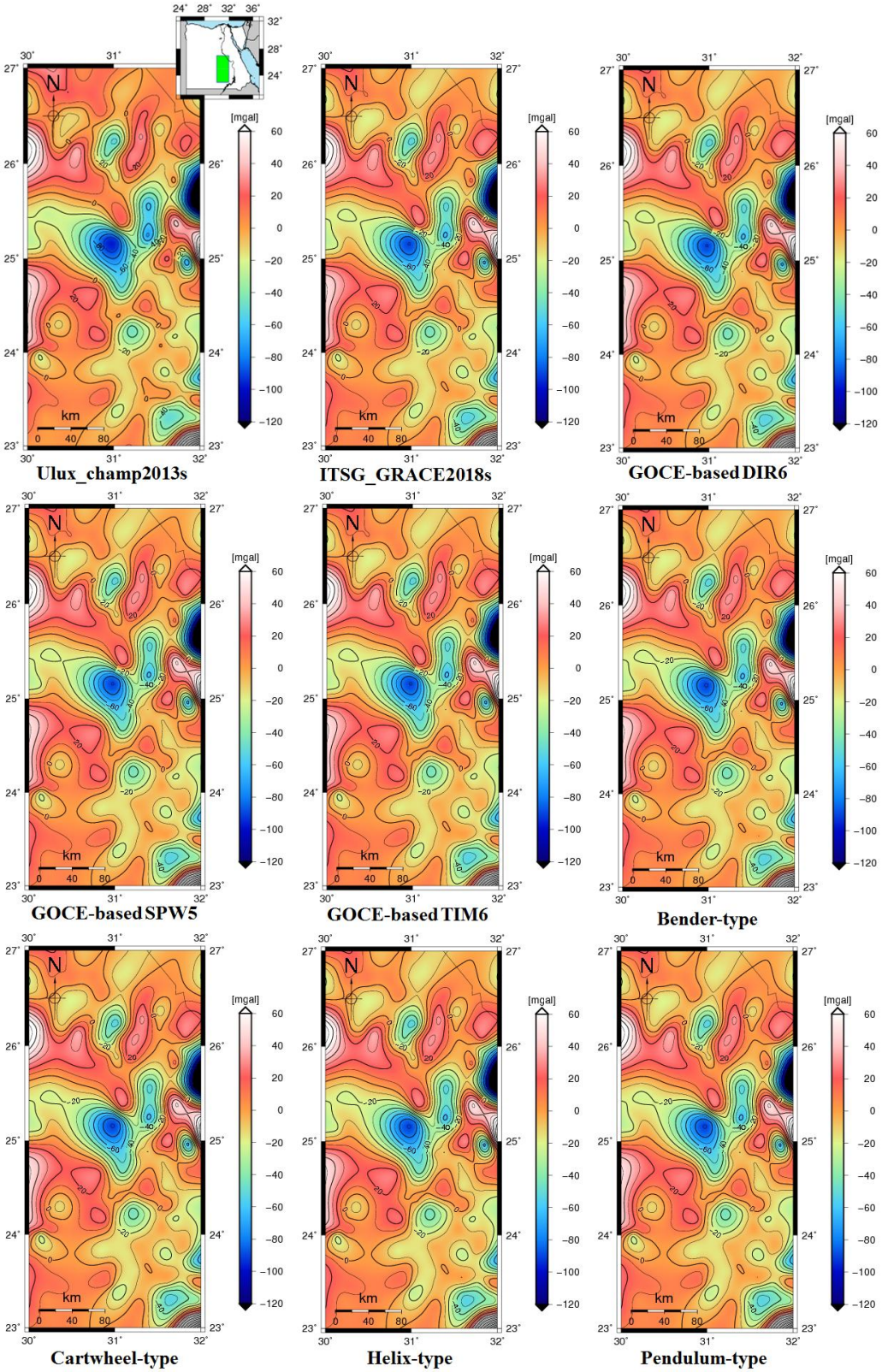

Figure 3. Residual free-air gravity anomalies (Δg_{res}) in [mGal] after the removal of the long, short and very-short wavelength gravity spectrum as represented by Equation (5).

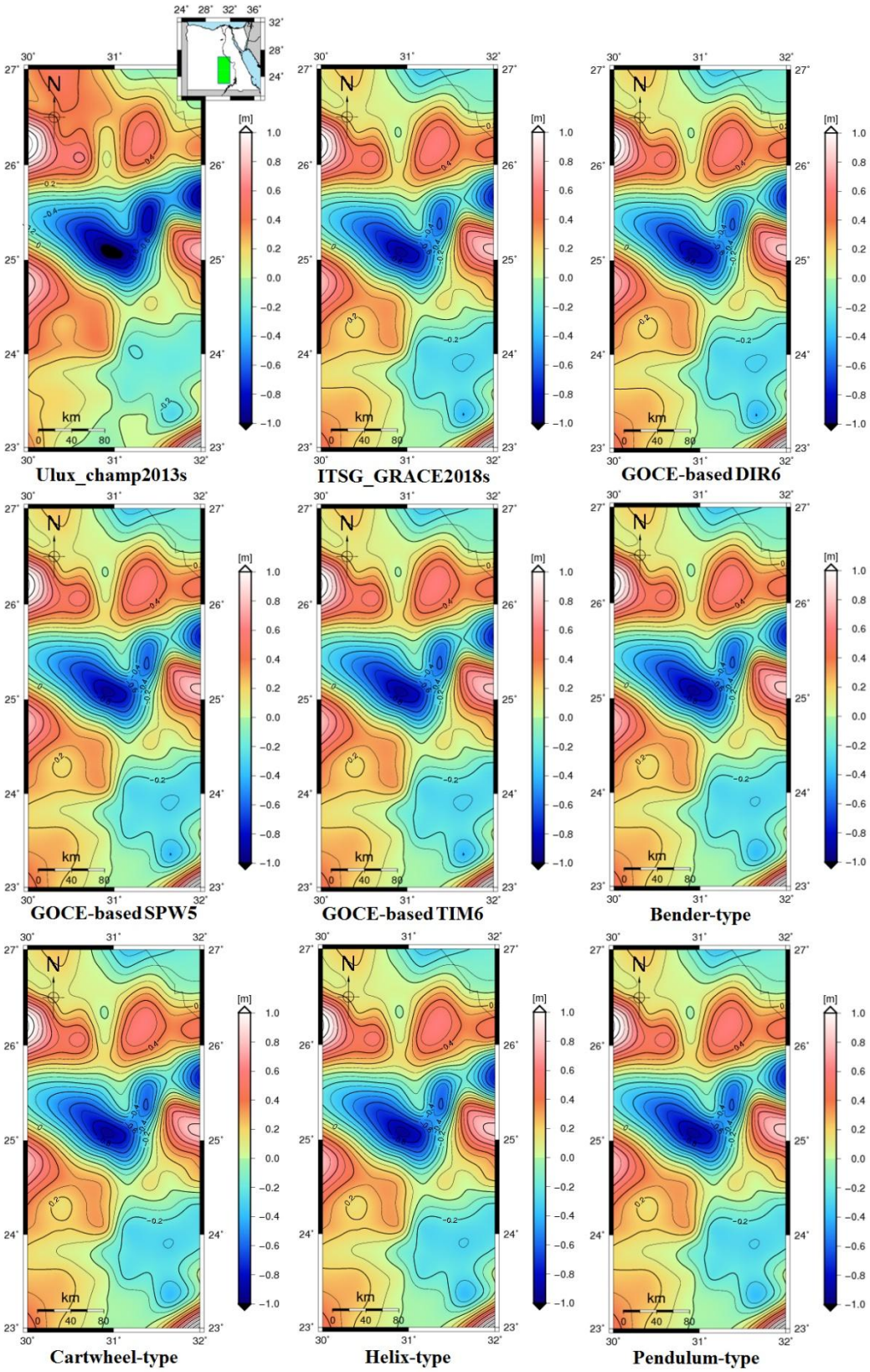

Figure 4. Residual height anomalies (ζ_{res}) in [m].

V. Conclusions

In this paper, numerous gravimetric quasi-geoid models for a selected zone of the Western Deseret of Egypt between 23°N to 27°N and from 30°E to 32°E have been estimated based on combined free-air anomalies from satellite-based of the previous and future gravity missions and ground based data using the fast Fourier transformation (1D-FFT) method. Regarding the satellite-based datasets, the free-air anomalies were derived from the long-wavelength of the gravity spectrum form the geopotential models of CHAMP-based ulux_champ2013s, GRACE-based ITG-GRACE2010s and GOCE-based GO_CONS_GCF_2_SPW_R5 (SPW5), GO_CONS_GCF_2_DIR_R6 (DIR6) and GO_CONS_GCF_2_TIM_R6 (TIM6). In addition, the free-air anomalies were derived from the long-wavelength of the gravity spectrum form future gravity missions; namely Bender-type, Cartwheel, Helix and Pendulum. For holding spectral consistency between the terrestrial- and satellite-based gravity anomalies, we have added the contribution of the short and very-short wavelength gravity signals beyond the applied maximum degree of GGMs (i.e. up to d/o 120) using the Eigen-6C4 (from d/o 121 – 720) and the remaining topography (RTM), respectively. Correspondingly, the residual free-air gravity anomalies interpolated on a grid of 0.25° x 0.25° resolution over the study are of the Western Desert of Egypt have been converted to the residual geoid heights applying the wong-gore modification of stokes' integral within the fast Fourier transformation (1D-FFT) process.

We can conclude that the long wavelength spectrum derived from geopotential models of future gravity missions, particularly the Bender-type; show a superiority in modelling the local geoid heights over selected region providing the least standard deviations in terms of residual gravimetric quasi-geoid heights of about 32.571 cm. The past gravity missions (CHAMP, GRACE and GOCE) provide relatively higher st. dev. of residual gravimetric quasi-geoid heights of about 36.51 cm for CHAMP, 32.62 for GRACE and between 32.62 to 32.64 for the GOCE geopotential models.

References

[1]. Anselmi, A., Cesare, S., Visser, P., Van Dam, T., Sneeuw, N., Gruber, T., Altes, B., Christophe, B., Cossu, F., Ditmar, P. Murboeck, M., Parisch, M., Renard, M., Reubelt, T., Sechi, G., Texieira Da Encarnacao, J.G. (2011). Assessment of a next generation gravity mission to monitor the variations of Earth's gravity field. ESA contract no. 22643/09/NL/AF, executive summary. Thales Alenia Space report SD-RP-AI-0721, March 2011.

[2]. Bender, P., Wiese, D., Nerem, R. (2008). A possible dual-GRACE mission with 90 degree and 63 degree inclination orbits. Paper Presented at Third International Symposium on Formation Flying. Eur. Space Agency, Noordwijk, Netherlands (23–25 April 2008).

[3]. Daras, I., Pail, R., Murböck, M., Yi, W. (2014). Gravity field processing with enhanced numerical precisionfor LL-SST missions. J Geod 89(2):99–110, https://doi.org/10.1007/s00190-014-0764-2.

[4]. Elsaka, B., (2010). Simulated Satellite Formation Flights for Detecting the Temporal Variations of the Earth's Gravity Field. Ph.D. Dissertation University of Bonn, Germany.

[5]. Elsaka, B., Kusche, J., Ilk, K.-H. (2012). Recovery of the Earth's gravity field from formation-flying satellites: temporal aliasing issues. Adv. Space Res. 50, 1534–1552. http://dx.doi.org/10.1016/j.asr.2012.07.016.

[6]. Elsaka, B., Raimondo, J.-C., Brieden, Ph., Reubelt, T., Kusche, J., Flechtner, F., Iran Pour, S., Sneeuw, N., Müller, J. (2014). Comparing seven candidatemission configurations for temporal gravity retrieval through full-scale numerical simulation. J. Geod. 88 (No. 1), 31–43. http://dx.doi.org/10.1007/s00190-013-0665-9.

[7]. Elsaka, B., Ilk, K.-H., Alothman, A. (2015). Mitigation of Oceanic Tidal Aliasing Errors in Space and Time Simultaneously Using Different Repeat Sub-Satellite Tracks from Pendulum-Type Gravimetric Mission Candidate. Acta Geophysica, vol. 63, no. 1, pp. 301-318, doi:10.2478/s11600-014-0251-4.

[8]. Elsaka, B. (2019). Spatio-Temporal Polar-Inclined Space Mission Architecture for a Refined Retrieve of the Earth's Gravity Field. World Journal of Engineering and Technology 7 (No. 4), 640-651.

[9]. ESA (1999). Gravity Field and Steady-State Ocean Circulation Explorer Mission. Report of European Space Agency for mission selection, the fourth candidate Earth explorer core missions, SP-1233, Nordwijk, Netherlands.

[10]. Flechtner, F., Dahle, C., Neumayer, K.H., König, R., Förste, Ch. (2010). The Release 04 CHAMP and GRACE EIGEN Gravity Field Models, In: Frank Flechtner, Thomas Gruber, Andreas Güntner, Mioara Mandea, Markus Rothacher, Tilo Schöne and Jens Wickert (Eds.): System Earth via Geodetic-Geophysical Space Techniques, Springer, ISBN 978-3-642-10227-1, doi.978-3-642-10228-8, pp 41 – 58.

[11]. Flechtner, F., Neumayer, K.H., Dahle, C., Dobslaw, H., Fagiolini, E., Raimondo, J.C., Guntner, A. (2016). What Can be Expected from the GRACE-FO Laser Ranging Interferometer for Earth Science Applications? Surv. Geophys., 37, 453–470.

[12]. Forsberg, R. and Tscherning, C.C. (2008). An Overview Manual for the GRAVSOFT Geodetic Gravity Field Modelling Programs, 2. Edition, National Space Institute (DTU-Space), Denmark, August.

[13]. Gabriel, A. and Goldstein, R. (1988). Crossed orbit interferometry: theory and experimental results from SIR-B. International Journal of Remote Sensing, Vol. 9, Issue 5, https://doi.org/10.1080/01431168808954901.

[14]. Haagmans, R., Siemes, C., Massotti, L., Carraz, O., Silvestrin, P. (2020). ESA's next-generation gravity mission concepts. Rend. Fis. Acc. Lincie, 31, 15– 25. https://doi.org/10.1007/s12210-020-00875-0.

[15]. Heiskanen, W.A. and Moritz, H. (1967). Physical Geodesy. WH Freeman and Company. San Francisco, CA.

[16]. Iran-Pour, S., Sneeuw, N., Daras, I., Pail, R., Murböck, M., Gruber, T., Tonetti, S., Cornara, S., Weigelt, M., Van Dam, T., Visser, P., de Teixeira da Encarnação, J. (2015). Assessment of satellite constellations for monitoring thevariations in earth gravity field - SC4MGV. ESA - ESTEC Contract No. AO/1-7317/12/NL/AF, Final Report.

[17]. Massonnet, D. (1998). Roue interférométrique. French patent no 339920D17306RS.

[18]. Nie, Y., Shen, Y., Chen, Q. (2019). Combination Analysis of Future Polar-Type Gravity Mission and GRACE Follow-On. Remote Sens. 2019, 11, 200.

[19]. Pail, R., Gruber, T., Abrykosov, P., Hauk, M., Purkhauser, A. (2018). Assessment of NGGM Concepts for Sustained Observation of Mass Transport in the Earth System. Presented at the GRACE/GRACE-FO Science Team Meeting, Potsdam, Germany, 10 October 2018. Available online: https://meetingorganizer.copernicus.org/GSTM-2018/GSTM-2018-10.pdf.

[20]. Pavlis, N.K., Holmes, S.A., Kenyon, S.C., Factor, J.K. (2012). The development and evaluation of the earth gravitational model 2008 (EGM2008), J Geophys. Res. 117(B04406): 1–38. doi:10.1029/2011JB008916.
[21]. Reigber, Ch. (1989). Gravity Field Recovery from Satellite Tracking Data, Lecture Notes in Earth Sciences, Theory of Satellite Geodesy and Gravity Field Determination, Eds. Sanso, Rummel , Springer.
[22]. Reigber, Ch., Schwintzer, P., Lühr, H. (1999). The CHAMP geopotential mission. Bolletino di Geofisica Teorica ed Applicata, Vol. 40:285289.
[23]. Saadon, A, El-Ashquer, M., Elsaka, B., El-Fiky, G. (2021). Determination of local gravimetric geoid model over Egypt using LSC and FFT estimation techniques based on different satellite- and ground-based datasets. Survey Review, doi.org/10.1080/00396265.2021.1932148.
[24]. Sharifi, M., Sneeuw, N., and Keller, W. (2007). Gravity Recovery capability of four generic satellite formations. In Proc. Kilicoglu, A. and R. forsberg (Eds.), Gravity Field of the Earth. General Command of Mapping, ISSN 1300-5790, Special issue 18, 211–216.
[25]. Sneeuw, N., Sharifi, M., Keller,W. (2008). Gravity recovery from formation flight missions. In: Xu, Peiliang, Liu, Jingnan, Dermanis, Athanasios (Eds.), VI Hotine-Marussi Symposium on Theoretical and Computational Geodesy. vol. 132. Springer, Berlin, Heidelberg, pp. 29–34.
[26]. Tapley, B. D., Bettadpur, S., Watkins, M., Reigber, Ch. (2004). The Gravity Recovery and Climate Experiment: Mission Overview and Early Results. Geophysical Research Letters, Vol. 31, 10.1029/2004GL019920.
[27]. Wiese, D., Folkner,W., Nerem, R. (2009). Alternative mission architectures for a gravity recovery satellite mission. J. Geod. 83, 569–581. http://dx.doi.org/10.1007/s00, 190-008-0274-1.
[28]. Wiese, D., Nerem, R., Han, S.-C. (2011). Expected improvements in determining continental hydrology, ice mass variations, ocean bottom pressure signals, and earthquakes using two pairs of dedicated satellites for temporal gravity recovery. J. Geophys. Res. 116, B11 405. http://dx.doi.org/10.1029/2011JB008375.
[29]. Wiese, D., Nerem, R., Lemoine, F., (2012). Design considerations for a dedicated gravity recovery satellite mission consisting of two pairs of satellites. J. Geod. 86, 81–98. http://dx.doi.org/10.1007/s00190-011-0493-8.
[30]. Wong, L. and Gore, R. (1969). Accuracy of Geoid Heights from Modified Stokes Kernels. Geophysical Journal International, 18, 81-91.

Basem Elsaka, et. al. "Determination of Local Quasi-Geoid Models using FFT Estimation Technique based on Combined Gravity Anomalies from CHAMP, GRACE, GOCE, Future Satellite Missions and in-Situ Gravity observations in Western Desert of Egypt."*IOSR Journal of Applied Geology and Geophysics (IOSR-JAGG)*, 10(1), (2022): pp 15-24.